CONF-800104--6

POWER TAKE-OFF ANALYSIS FOR DIAGONALLY CONNECTED MHD CHANNELS

by

Yen-Cheng and Ezzat D. Doss

MASTER

Prepared for

AIAA 18th Aerospace Sciences Meeting

Pasadena, California

January 14-16, 1980

UofC-AUA-USDOE

ARGONNE NATIONAL LABORATORY, ARGONNE, ILLINOIS

Operated under Contract W-31-109-Eng-38 for the

U. S. DEPARTMENT OF ENERGY

The facilities of Argonne National Laboratory are owned by the United States Government. Under the terms of a contract (W-31-109-Eng-38) among the U. S. Department of Energy, Argonne Universities Association and The University of Chicago, the University employs the staff and operates the Laboratory in accordance with policies and programs formulated, approved and reviewed by the Association.

MEMBERS OF ARGONNE UNIVERSITIES ASSOCIATION

The University of Arizona
Carnegie-Mellon University
Case Western Reserve University
The University of Chicago
University of Cincinnati
Illinois Institute of Technology
University of Illinois
Indiana University
The University of Iowa
Iowa State University
The University of Kansas
Kansas State University
Loyola University of Chicago
Marquette University
The University of Michigan
Michigan State University
University of Minnesota
University of Missouri
Northwestern University
University of Notre Dame
The Ohio State University
Ohio University
The Pennsylvania State University
Purdue University
Saint Louis University
Southern Illinois University
The University of Texas at Austin
Washington University
Wayne State University
The University of Wisconsin-Madison

POWER TAKE-OFF ANALYSIS FOR DIAGONALLY CONNECTED MHD CHANNELS **

Yen-Cheng Pan and Ezzat D. Doss*
Argonne National Laboratory
Argonne, Illinois 60439

Abstract

The electrical loading of the power take-off region of diagonally connected MHD channels is investigated by a two-dimensional model. The study examines the loading schemes typical of those proposed for the U-25 and U-25 Bypass channels. The model is applicable for the following four cases: 1) connection with diodes only, 2) connection with diodes and equal resistors, 3) connection with diodes and variable resistances to obtain a given current distribution, and 4) connection with diodes and variable resistors under changing load. The analysis is applicable for the power take-off regions of single or multiple-output systems. The general behaviors of the current and the potential distributions in all four cases are discussed. The analytical results are in good agreement with the experimental data. It is found possible to design the electrical circuit of the channel in the take-off region so as to achieve a fairly even load current output under changing total load current.

Nomenclature

A	cross sectional area of the channel
$\vec{B}$	magnetic field
$\vec{E}$	electric field
H	height of the channel (in y-direction)
I	load current
I_s	local short circuit current
i_n	current in the nth leadout
i	$= i_n/\delta = dI/dx$
$\vec{J}$	current density
$\dot{m}$	mass flow rate
Q	$= (1 + \beta^2)/\sigma$
R	$= R_\ell \delta$
R_ℓ	resistance per unit length of the channel
R_n	resistance in the nth electric leadout
T_o	stagnation temperature at channel inlet
u	velocity in x-direction
x, y, z	Cartesian coordinates
β	Hall parameter
δ	pitch of the window frame
ϕ	electric potential
θ	diagonalization angle
σ	conductivity

$$\langle\beta\rangle = 1/H \int_0^H \beta \, dy$$

$$\langle\sigma\rangle = 1/H \int_0^H \sigma \, dy$$

$$\langle Q\rangle = 1/H \int_0^H Q \, dy$$

$$\langle u\rangle = 1/H \int_0^H u \, dy$$

* Member AIAA **

I. Introduction

The diagonal loading scheme for a magnetohydrodynamic (MHD) channel was first proposed by De Montardy[1] and Dicks.[2] Dicks proposed his diagonal conducting wall (DCW) channel, which consisted of window frame-like electrode modules insulated from each other. Subsequently, the channel performance was extensively studied.[3,4] Since then, the DCW channel has received a great deal of attention. Experiments on the DCW channel have shown high performance and durability. This type of channel construction has been adopted for the U.S./U-25[5] and U-25 Bypass[6] channels.

The DCW channel is also noted for its simple design of the power take-off region. An example of the loading schemes typical of that for the U-25 Bypass channel is depicted in Fig. 1. The electric leadout from each frame is connected to a diode, or a diode and a resistor before it is connected to the bus bar. The current from all the leads is then transmitted to a dc-ac inverter, where the external load is applied.

An important problem related to the design of the power take-off region is the end effect, which was investigated in Refs. 7-12. These articles examine the internal electric fields and eddy current losses caused by the change of load current and the magnetic field. It is generally concluded that the power take-off electrodes should be placed near the ends of the channel, where the magnetic field is attenuating, in order to reduce the eddy current loss. Wherever the power take-off section spans across several electrodes, another area of interest should be considered: the current distribution among the current leadouts and their optimum locations. Dzung[7] and Ishikawa[12] discussed the ballast resistors required for obtaining equal current in each frame. Levi[13] solved the current distributions in the electric leadout connections with diodes or diodes and equal resistors. The study is, however, based on a one-dimensional model, constant average plasma properties, and constant velocity field assumptions, and does not handle the intermediate multiple-loading power take-off regions.

The subject paper uses a two-dimensional model[14] to investigate the following cases: 1) connection with diodes only, 2) connection with diodes and equal resistors, 3) connection with diodes and variable resistances to obtain a given current distribution, and 4) connection with diodes and variable resistors under changing loads. The analysis is general and is applicable also for intermediate multiple-load connections, which has not been investigated previously.

II. Governing Equations

The two dimensional MHD channel model described in Ref. 14 is used in this study. The model solves the two-dimensional compressible turbulent flow equations by an implicit finite differencing scheme.

The electric field, $\vec{E}$, and the current density $\vec{J}$ in the channel are obtained by solving Ohm's law and the Maxwell equations:

$$\vec{E} + \vec{U} \times \vec{B} = \frac{1}{\sigma} \vec{J} + \frac{\beta}{\sigma} \vec{J} \times \vec{B}.$$

$$\nabla \times \vec{E} = 0$$

$$\nabla \cdot \vec{J} = 0 \qquad (1)$$

To simplify the analysis, the infinite segmentation assumption[14], has been used; the following equations are obtained.

$$E_x = \frac{\langle Q \rangle I - A(\langle \beta \rangle + \tan\theta)\ \langle u \rangle B}{A(\tan^2\theta - \langle \beta \rangle^2 + \langle \sigma \rangle \langle Q \rangle)} ,$$

$$J_y = \frac{(\langle \beta \rangle - \tan\theta)\ E_x - \langle u \rangle B}{\langle Q \rangle} , \qquad (2)$$

for the short circuit condition,

$$E_x = 0,$$

$$I = I_s = \frac{A(\langle \beta \rangle + \tan\theta)}{\langle Q \rangle} \langle u \rangle B. \qquad (3)$$

Therefore, the equation for E_x can be written as

$$E_x = R_\ell(x)\ (I - I_s) , \qquad (4)$$

where

$$R_\ell(x) = \frac{\langle Q \rangle}{A(\tan^2\theta - \langle \beta \rangle^2 + \langle \sigma \rangle \langle Q \rangle)} .$$

A typical schematic loading diagram for two adjacent frames is shown in Fig. 2. The current in the electric leadout from each frame can be related to the interframe voltage by the difference equation,

$$i_{n+1} R_{n+1} - i_n R_n = \delta E_x . \qquad (5)$$

Using the Taylor series expansion, Eq. 5 becomes

$$\frac{d(iR)}{dx} = E_x = R_\ell (I - I_s) . \qquad (6)$$

In the following sections, the power take-off region is considered to extend from $X = X_1$ to $X = X_2$, where the load current changes from $I = I_1$ to $I = I_2$. The power take-off section may be located at the inlet, exit, or intermediate regions of the channel.

The solution to the power take-off problem is subjected to the following constraints, if diodes are present,

$$i \geq 0 \qquad (\text{if } I_2 > I_1) ,$$

$$i \leq 0 \qquad (\text{if } I_2 < I_1) . \qquad (7)$$

The boundary conditions are,

$$I = I_1 \qquad \text{at } X = X_1 ,$$

$$I = I_2 \qquad \text{at } X = X_2 . \qquad (8)$$

Eqs. (6), (7), and (8) are coupled with the gasdynamic and electrical equations described in Ref. 14, to form the complete set of governing equations.

III. Connection with Diodes Only

In this case, R = 0 and Eq. (6) becomes

$$E_x = 0,$$

$$I = I_s. \qquad (9)$$

Hence, the load current inside the channel in the power take-off region assumes the local short circuit current subject to Eq. (8). The current and potential distributions typical of the U-25 channel are shown in Figs. 3 to 6. In these plots, X_s denotes the location where the short circuit current, I_s, is equal to the load current, I. The channel operating conditions used in these calculations are given in Table I.

In the inlet power take-off region [(a) and (b) of Fig. 3], the first leadout electrode always picks up the channel local short circuit current. It can be seen in Fig. 3 that the current in the first leadout electrode is quite high for the U-25 channel. This is because of the relatively high value of the magnetic field; however, most of this current will be picked up by the nozzle. The next leadout electrode carries the difference between the local short circuit current and the previous I_s value, so that the sum of the leadout currents up to that point is equal to the channel local short circuit current, until X_2 or X_s is reached. If $X_2 \geq X_s$ (Fig. 3b), the diodes located at $X > X_s$ will be blocking, and the Hall potential of the channel will start to increase. In this case, the leadout currents follow a smooth curve, except for the first one. If $X_2 < X_s$ (Fig. 3a), the last power take-off electrode picks up an extra current equal to $(I_2 - I_s)$ as compared to the electrode in the same location in Fig. 3b. Consequently, the Hall potential starts reversing and the channel absorbs power. Finally, the Hall field stops reversing at X_s; however, the Hall potential is still negative, and it returns to zero later, at $X > X_s$.

At the exit power take-off region, if the location of the diodes starts at $X < X_s$ (Fig. 4b), only the diodes at $X \geq X_s$ will be conducting. Each electrode carries a current equal to the difference between the local channel short circuit current, I_s, at this electrode and the previous one until X_2 is reached. The last electrode then picks up the short circuit current at $X = X_2$. If the location of diodes starts at $X > X_s$ (Fig. 4a), the Hall field reversal starts at $X = X_s$ and stops at $X = X_1$. In this case, the leadout

electrode located at $X = X_1$ picks up an additional current equal to $(I_1 - I_s)$. This situation again reduces the electric power produced by the channel.

Two typical cases of intermediate power take-off regions are shown in Figs. 5 and 6, where the local channel short circuit current is increasing or decreasing, respectively. In Fig. 5a, the load current, I_1, is greater than the local short circuit current at $X < X_{s1}$; therefore, potential field reversal occurs in that region. At $X = X_1$, the load current begins to assume the short circuit current until $X = X_2$, where the load current jumps to the value, $I = I_2$. The last leadout electrode picks up a large current and the potential field reverses. If I_1 is reduced and X_2 is shifted downstream past $X = X_{s2}$, there will be no potential field reversal, as shown in Fig. 5b. It is also possible to have the power take-off region moved downstream, so that X_1 is greater than X_{s2}. In that case, the load current jumps to $I = I_2$ at $X = X_1$, but with no field reversal. This case is not plotted; however, it can exist.

For the intermediate power take-off regions where the load current is decreasing, the results are plotted in Fig. 6. In Fig. 6a, the power take-off region is located between $X_1 > X_{s1}$ and $X_2 < X_{s2}$. In this case, Hall-potential field reversal occurs at both ends of the power take-off region, and the end leadouts pick up large currents. If the power take-off region is extended so that $X_1 < X_{s1}$ and I_2 is reduced, there will be no field reversal, as shown in Fig. 6b. If the power take-off region is moved upstream so that $X_2 < X_{s1}$, the diodes located at $X < X_2$ will be blocking. The load current will jump from I_1 to I_2 at the last electrode at $X = X_2$, however, with no field reversal.

IV. Connection with Diodes and Equal Resistors

If the resistors used in the power take-off regions are the same, Eq. 6 becomes,

$$\frac{d^2I}{dX^2} = \frac{E_x}{R} = \frac{R_\ell}{R}\,(I - I_s). \qquad (10)$$

A qualitative description of the load current distribution can be obtained by dividing the I-X domain into two regions as shown in Fig. 7. In the upper region, $I > I_s$; therefore, $E_x > 0$ and $d^2I/dX^2 > 0$. Hence, the load current curve should be concave. In the lower region, however, $I < I_s$; therefore $E_x < 0$ and $d^2I/dX^2 < 0$, and the load current curve should be convex.

An additional constraint on the load current distribution is imposed by the diodes. For example, near the channel inlet, in the region where the load current is increasing, $i = dI/dX \geq 0$. Therefore, the current distribution must assume the solid lines of the upper and lower curves in Fig. 7, depending on whether $I > I_s$ or $I < I_s$, respectively. Because the current measured in each leadout is equal to $\delta x\, di/dX$, the current distribution in the upper region results in increasing current distribution along the leadouts (i increasing), accompanied by a field reversal. The current distribution in the lower region results in a decreasing current distribution along the leadouts (i decreasing), with no field reversal. In the region of decreasing load current (at the exit power take-off region), the current distribution assumes the dashed line in Fig. 7, also depending on whether $I > I_s$ or $I < I_s$. In this case, a decreasing current distribution along the leadouts is accompanied by field reversal (top curve, $I > I_s$), whereas there is no field reversal for an increasing individual current distribution along the leadouts (bottom curve, $I < I_s$).

Numerical solutions for the current and potential distributions typical of the U-25 Bypass channel are shown in Figs. 8 to 11. The dimensions and operating conditions used in the calculations are given in Table II. If the power take-off region is located between frames 5 and 23, the results are shown in Fig. 8a for $I_2 = 155$ A. It is noted that the short circuit current near the channel inlet is very small, because the magnetic field is small at the channel inlet. As a result, the load current in frames 5 through 12 is greater than the short circuit current. Therefore, the electrical potential decreases and the leadout currents increases. In frames 13 through 23, the load current is less than the short circuit current. Therefore, the Hall potential starts increasing and the leadout currents starts decreasing at frame 13. At frame 17, the load current curve is tangent to $I = I_2$ line. The diodes at frames 17 to 23 are blocking. If the power take-off region is moved to frames 5 through 16 (Fig. 8b) the load current is greater than the short circuit current in all locations for $I_2 = 209$ A, and this is accompanied by axial field reversal.

If the channel inlet power take-off region is moved downstream, the expected current and potential distribution are as shown in Fig. 9. The qualitative description represented in this figure is also applicable to intermediate power take-off connections if the load current is increasing. In this case, higher U X B results in a higher induced emf and higher short circuit current. If the power take-off region is located between frames 8 through 19, Fig. 9a indicates that the load current is smaller than the short circuit current in frames 8 to 10 and is greater than the short circuit current in frames 11 to 19. Therefore, field reversal occurs in frames 11 to 19, accompanied by an increasing leadout current distribution. If the power take-off region is moved farther downstream to frames 12 through 23 (Fig. 9b), the load current is less than the short circuit current at all locations; hence, the leadout current is decreasing from frame 12 to frame 23, and there is no axial field reversal. Fig. 10 presents the current distribution for three different power take-off locations where the total load current is constant. It is noted that the current in the first (upstream) leadout electrode increases while the current in the last (downstream) leadout decreases. As noted by the change in current distribution, the chance for electric field reversal is reduced if the power take-off region is moved downstream.

The electrical current and potential distributions in the region of decreasing load current (channel exit or intermediate region) is the mirror image of the distribution in the region of increasing load current. Therefore, similar argument can be applied and the results are as shown in Figs. 11 and 12.

Most of the situations discussed in the foregoing section were observed experimentally during the several tests that were conducted on the U-25 Bypass channel[6,15,16]. The analytical results for the inlet power take-off region were found to be in good agreement with the experimental data[16] as shown in Fig. 13. The exit power take-off region was not investigated analytically because of the difficulty encountered in modeling the oblique shocks that are present near the channel exit. However, the qualitative results of this model are expected to hold, also, at the channel exit power take-off region.

V. Connection with Diodes and Variable Resistors

With diodes and variable resistors, the power take-off region can be designed to have any given load current distribution. The general features of the design and off-design conditions can be examined by studying the special case of a linear load current distribution. The general case of nonlinear current distribution can then be looked at as piecewise linear distribution.

a. Equal Current for Each Frame (Design Point)

If the channel loading is designed to have equal leadout current for each frame, Eq. (6) has the solution

$$R(x) = \frac{1}{i}\int_{x_i}^{x} R_\ell\,(iX - I_s)\,dX + R_o\,, \qquad (11)$$

where R_o is an arbitrary constant. In order to minimize the dissipated power loss, R_o is determined to be

$$R_o = -\min_{x_1 \to x_2}\left[\frac{1}{i}\int_{x_1}^{x} R_\ell(iX - I_s)\,dX\right]. \qquad (12)$$

Actually, R_o is determined so that the minimum value of R is zero.

Depending on the channel short circuit current and the load current distributions, four typical resistance variations can exist. These variations, together with their corresponding load current distributions, are shown in Fig. 14. It is interesting to compare Fig. 14 with Figs. 8-11 (where the resistances are kept the same). For example, in Fig. 8a, leadout current is maximum near the middle of the power take-off section. In order to redistribute the current evenly among neighboring electrodes, the resistance should be increased at the middle and decreased near the ends of the power take-off region. This results in the resistance distribution given in Fig. 14a. The behavior of the other curves shown in Fig. 14 can be explained in a similar manner.

b. Off-Design Current and Potential Distribution

In this case, Eq. (6) can be rearranged to become

$$\frac{di}{dx} = \frac{R_\ell}{R}\,(I - I_s) - \frac{i}{R}\frac{dR}{dx}\,. \qquad (13)$$

The first part of the right hand side of Eq. (13) is the same as that of Eq. (10) for equal resistors. From this equation, it can be seen that the leadout current distribution no longer depends only on whether I is greater or less than I_s; rather, an additional contribution is made by the rate of change of the resistance. A negative slope tends to distribute more current in the downstream leadouts. The contribution of the resistance term is further enhanced because of the typical high value of i/R, if the slope of the resistance is negative.

Numerical solutions for the typical redistribution of the load current among the power take-off frames at off-design operating conditions are shown in Fig. 15, a through d, corresponding to the cases shown in Figs. 14a-14d. In Fig. 14a, the resistances increase from frame 5 to frame 17 and decrease from frame 18 to frame 23. As a result, when the loading increases, the current distribution increases slowly from frame 5 to frame 17, but increases faster from frame 18 to 23. The effect is enhanced by the low resistance in the last frame. Therefore, the current change is mostly concentrated in the last frame, no. 23, as shown in Fig. 15a, where a value of 60 A is picked by this frame, whereas about 10A is picked by each other frame.

In Fig. 14b, the resistances increase from frame 5 to frame 16. Both the positive slope of the resistance curve and the high resistance near frame 16 tend to flatten the load current curves. Therefore, the current distributions in the power take-off regions stay reasonably uniform as the total load current varies.

In Fig. 14c, the resistance drops to zero at frame 11. Hence, any amount of current can flow through the 11th leadout without disturbing the voltage balance of frames 8 to 10. The change of current in the 10th frame only affects the downstream leadouts. Therefore, when the loading increases, the currents in frames 8 to 10 remain essentially unchanged. Because the resistance is increasing from frame 12 to 19, the variation of the current distribution is relatively uniform, as shown in Fig. 15c.

In Fig. 14d, the resistance decreases from 2.1 ohm at frame 12 to zero at frame 23. If the loading is increased in this case, the current is concentrated in frame 23, as shown in Fig. 15d, because of the negative slope of the resistance curve and because there is no ballast resistance at frame 23. In order to reduce the high current in the last frame and to minimize field reversal, it is necessary to move the power take-off region farther downstream, so that the off-design load current will be less

than the short circuit current. In this case, the first part of the right hand side of Eq. (13) will tend to reduce the current in the last leadout.

VI. Summary And Conclusions

1. A model has been developed for analysis of the leadout load current distribution in the power take-off regions of diagonally connected MHD channels. The developed model is applicable for external connections with diodes only, diodes with equal resistors, and diodes with variable resistors. The model can be used for the power take-off regions of single-as well as multiple-output systems.

2. The developed model is coupled to a two-dimensional MHD channel flow model that solves for the internal gasdynamic and electrical variables. Despite the limitations of the infinite segmentation assumption used in the internal model near the end regions of MHD channels, Equations (6)-(8) are quite general and are not limited by the internal modeling of the channel. The model can, therefore, be coupled to any other formulation that solves the MHD channel internal problem.

3. The analytical results of this model as applied to the U-25 Bypass channel agree, quantitatively, very well with the experimental data for the current distribution in the power take-off reigon. Therefore, despite of the simplified assumption used in the channel internal electrical solution, the subject model can not only yield qualitive trends that may aid the channel designers of the power take-off regions, but can also give quantitative results.

4. If only diodes are used in the power take-off region, it is important to extend the take-off connection beyond the point where the local short circuit current is equal to the highest load current expected. Failure to do so will result in large current in the end leadouts, accompanied by field reversal and loss of power.

5. If diodes and equal resistors are used in the power take-off region, the general behavior is as follows:

a) An increasing leadout current distribution in the inlet power take-off region and an decreasing lead-out current distribution in the exit power take-off region will be accompanied by Hall field reversal, and vice versa.

b) If the front power take-off region with fixed number of leadouts is shifted downstream in the channel, the current in the first (upstream) few leadouts increases ,whereas the current in the last (downstream) few leadouts decreases. This shift, in general, reduces the chance of field reversal; however, excessive shift of the take-off region downstream can result in loss of power. A general criterion is to stop where the downstream leadout current becomes close to zero. The rear power take-off region can be viewed as the mirror image of the front power take-off region.

6. Diodes and unequal resistors can be used to design for any given load current distribution. One criterion for this design is to have a reasonably even current distribution at both design and off-design operating conditions. It is noted that, in general, an increasing resistance distribution tends to even out the leadout current distribution, whereas a decreasing resistance distribution leads to large current in the last frame at off-design conditions. For a decreasing resistance distribution, it is advisable to have both design and off-design load currents less than the short circuit current.

Acknowledgement

The authors wish to thank their colleagues E. Pierson and S. Zwick for their helpful discussions.

Table I

U-25 Channel Operating Conditions
(used in the analysis)

Channel Dimensions:

Height:	inlet 0.732 m, exit 1.189 m
Width:	inlet 0.358 m, exit 0.645 m
Length:	7.144 m
Magnetic field:	2 T maximum
Mass flow rate:	33 kg/s
Fuel:	CH_4
Oxygen enrichment:	40 vol %
Oxidizer preheat temperature:	1200°C
Stoichiometric ratio	1.0
Seed fraction	1 mass % K as K_2CO_3 solution; K_2CO_3/H_2O = 1:1 by wt

Table II

U-25 Channel Operating Conditions
(used in the analysis)

Channel Dimensions:

Height:	inlet 0.154 m, exit 0.275 m
Width:	inlet 0.154 m, exit 0.275 m
Length:	5 m
Magnetic field:	5 T maximum
Mass flow rate:	3.2 kg/s
Fuel:	CH_4
Oxygen enrichment:	40 vol %
Oxidizer preheat temperature:	800°C

Stoichiometric ratio 1.0

Seed Fraction 1 mass % K as K_2CO_3 solution; K_2CO_3/H_2O = 1:1 by wt

REFERENCES

1. A. de Montardy, "MHD Generators with Series-Connected Electrodes," Proceedings of the International Symposium on MHD Electrical Power Generation, Paper No. 9, Sept. 6-8, 1962.

2. J. B. Dicks, "Design and Operation of Open Cycle Hall Current Neutralized MHD Accelerators and Generators with Diagonal Conducting Strip Walls," Proceedings of the 5th Symposium on Engrg. Aspects of MHD, MIT, Cambridge, Massachusetts, April 1-2, 1964.

3. J. B. Dicks, et al, "Characteristics of a Family of Diagonal Conducting Wall MHD Generators," Proceedings of 8th Symposium on Engrg. Aspects of MHD, March 28-30, 1967, p. 46-54.

4. J. B. Dicks, et al, "Theoretical and Experimental Studies of Two-Terminal MHD Generators," Proceedings, 4th International Conference on MHD Electrical Power Generation, July 24-30, 1968, p. 2719-2741.

5. T. R. Brogan, J. A. Hill, R. M. Goff, and N. Diatchenko, "Design of a Single Output MHD Generator for the U.S.S.R. U-25 Installation," U.S./U.S.S.R. MHD Colloquium, October 5-6, 1978, p. 223-246.

6. "U.S./U.S.S.R. Cooperative Program in Open Cycle MHD Electrical Power Generation, Joint Test Report No. 1," ANL-IVTAN/MHD-78-JT1, April, 1978.

7. L. Dzung, "The Magnetohydrodynamic Generator with Hall Effect at the Duct Ends," Brown Boveri Review, Vol. 49, 1962, p. 211.

8. W. T. Norris and J. B. Heywood, "End Region of a Single-Load Cross- Connected MHD Generator," Proceedings IEE, Vol. 115, 1968, p. 555.

9. O. Sonju and J. Teng, "Further Analytical Investigations of MHD Generator Performance," Proceedings of 12th Symposium on Engrg. Aspects of MHD, 1972, p. II.3.

10. J. C. Cutting, C. D. Maxwell, and R. T. Ling, "Calculation of End Effects in Open-Cycle MHD Power Generators," Proceedings of 16th Symposium on Engrg. Aspects of MHD, 1977, p. VII.4.21-26.

11. M. Ishikawa, "Two Dimensional Analysis of End Effects in Diagonal Type MHD Generator," Energy Conversion, Vol. 17, 1977, p. 113.

12. M. Ishikawa and Y. Hattori, "Effects of Position of Output Electrodes in Entrance Region of Open-Cycle Diagonal Type MHD Generator," Energy Conversion, Vol. 18, 1978, p. 155-161.

13. Levi, E., Private Communication, June 15, 1979.

14. E. Doss, H. Geyer, Z. El-Derini, and R. K. Ahluwalia, "Two-Dimensional MHD Channel Design," presented at the Winter Annual Meeting of ASME, Dec. 10-15, 1978.

15. "U.S./U.S.S.R. Cooperative Program in Open-Cycle MHD-Electrical Power Generation, Joint Test Report No. 2," ANL-IVTAN-JT2, April, 1979.

16. "U.S./U.S.S.R. Cooperative Program in Open-Cycle MHD Electrical Power Generation, Joint Test Report No. 3," ANL-IVTAN-JT3, to be published.

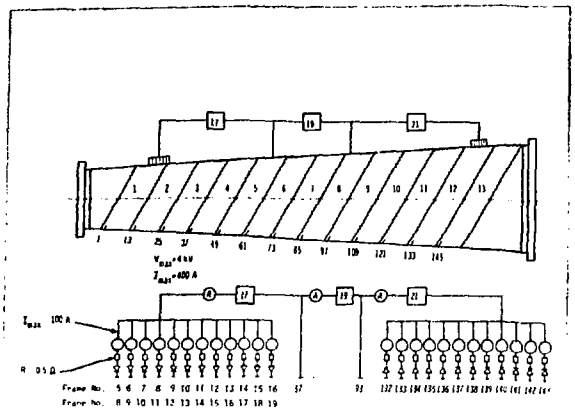

Fig. 1 Electrical loading schematic for the U-25 Bypass channel

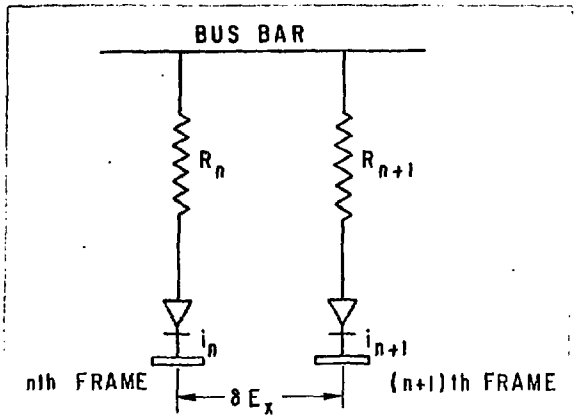

Fig. 2 A schematic diagram for a typical loading section

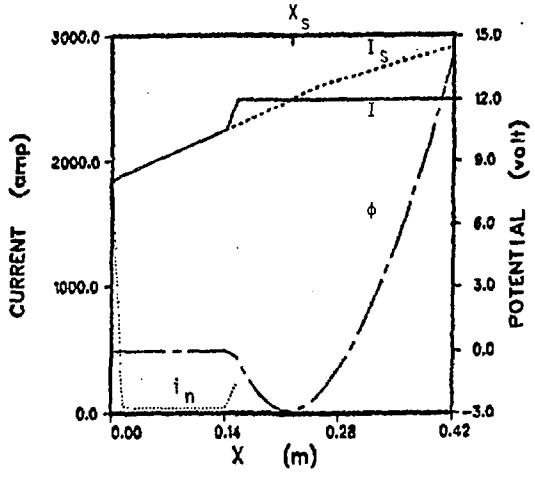

(a) I_1=0 at X=0; I_2=2500 at X_2=0.154

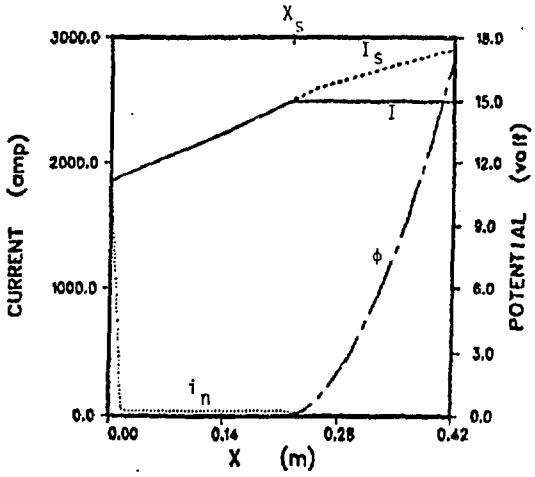

(b) I_1=0 at X_1=0; I_2=2500 at X=0.42

Fig. 3 Electrical current and potential distribution for the power take-off region with diodes only (at the channel inlet)

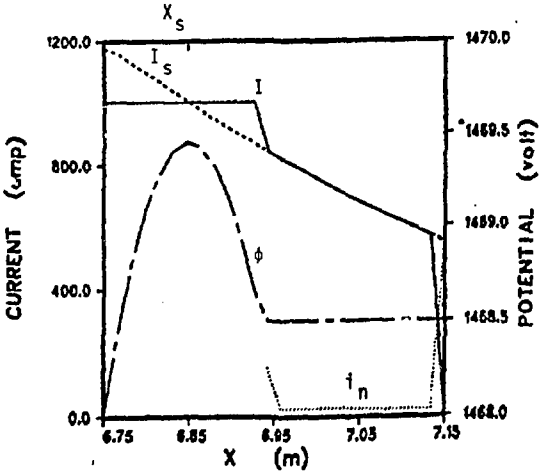

(a) I_1=1000 at X_1=6.942; I_2=0 at X_2=7.15

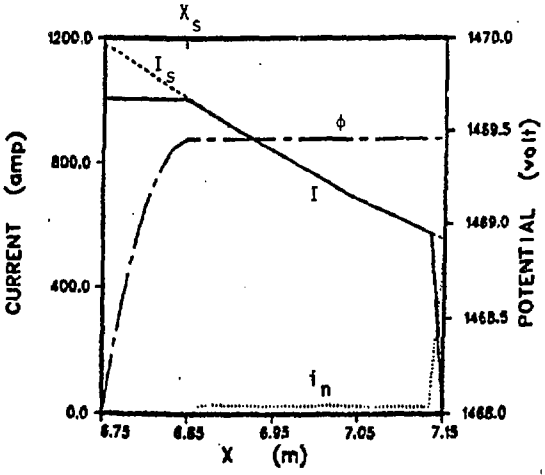

(b) I_1=1000 at X_1=6.75; I_2=0 at X_2=7.15

Fig. 4 Behavior of the power take-off region with diodes only (at the channel exit)

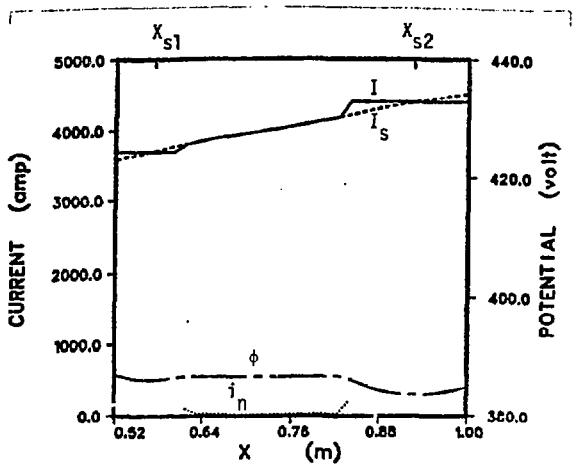

(a) I_1=2700 at X_1=0.648; I_2=4400 at X_2=0.84

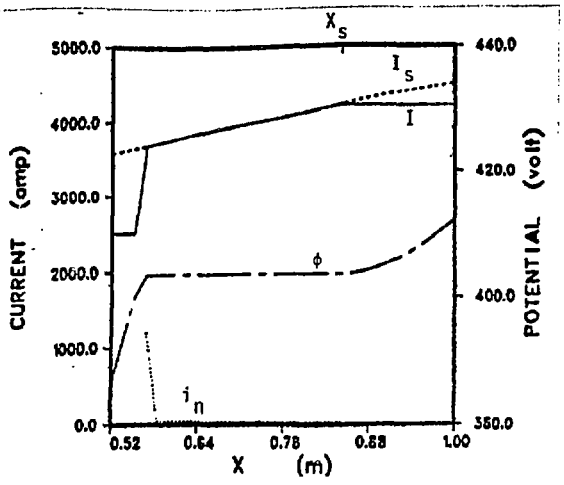

(b) I_1=2500 at X_1=0.568; I_2=4200 at X_2=1.0

Fig. 5 Behavior of the mid-channel power take-off connection with diodes only (increasing I_s)

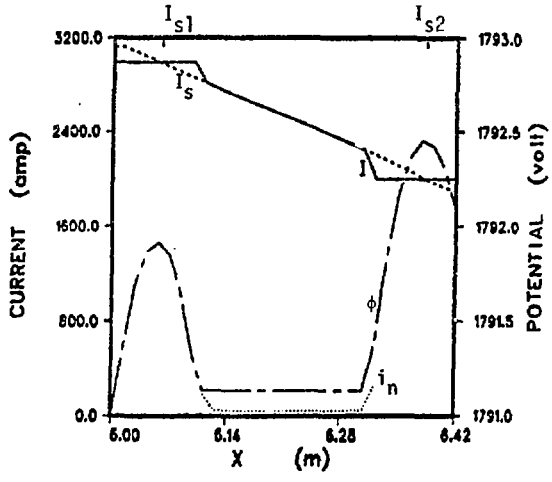

(a) I_1=3000 at X_1=6.112; I_2=2000 at X_2=6.322

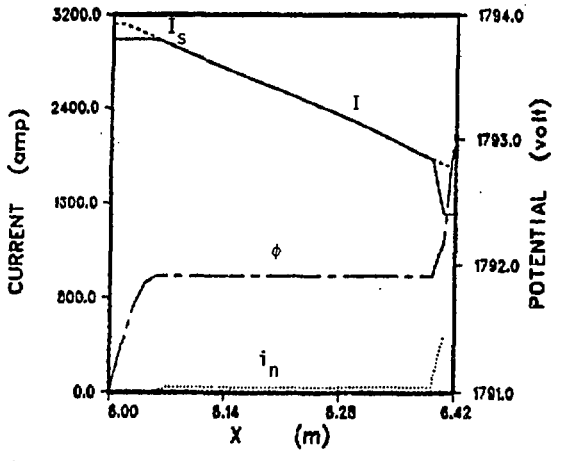

(b) I_1=3000 at X_1=6.0; I_2=1500 at X_2=6.406

Fig. 6 Behavior of the mid-channel power take-off connection with diodes only (decreasing I_s)

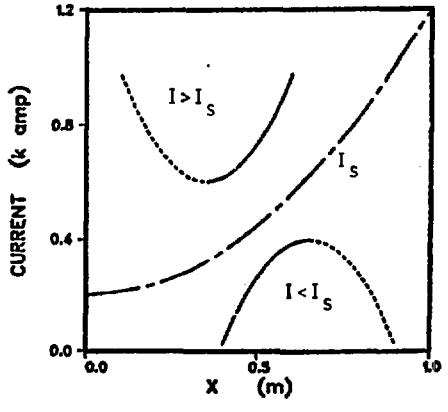

Fig. 7 Load current distribution in the power take-off region for connections with diodes and equal resistors

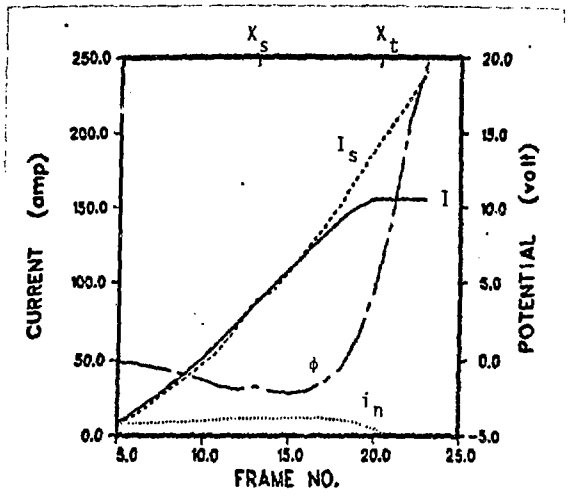

(a) I_1=0 at frame 5; I_2=155 at frame 23

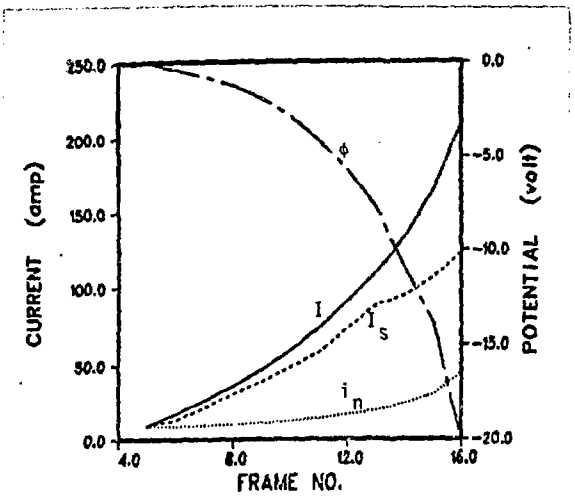

(b) I_1=0 at frame 5; I_2=210 at frame 16

Fig. 8 Electrical current and potential distributions for the power take-off region with diodes and equal resistors (channel inlet)

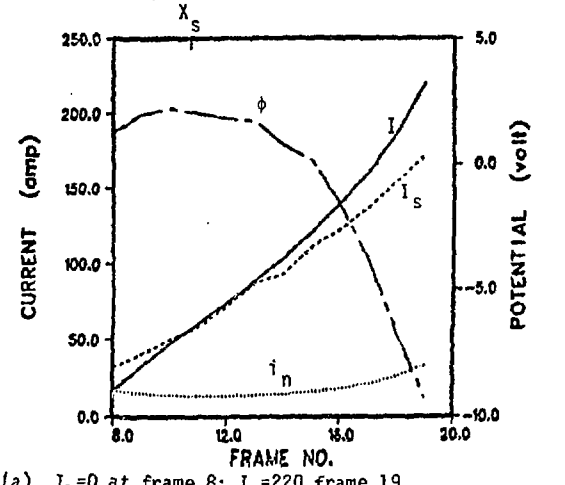

(a) I_1=0 at frame 8; I_2=220 frame 19

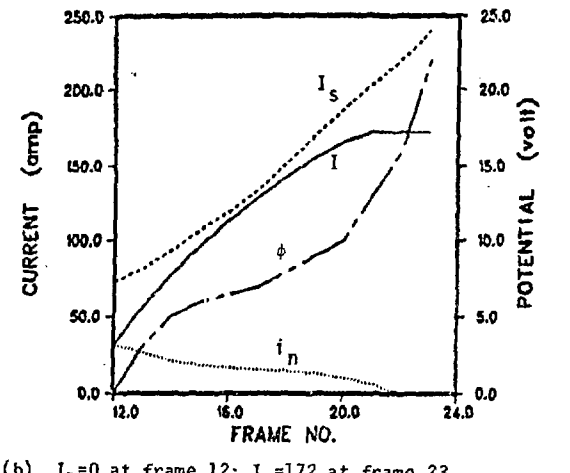

(b) I_1=0 at frame 12; I_2=172 at frame 23

Fig. 9 Behavior of the power take-off region with diodes and equal resistors (inlet or intermediate section)

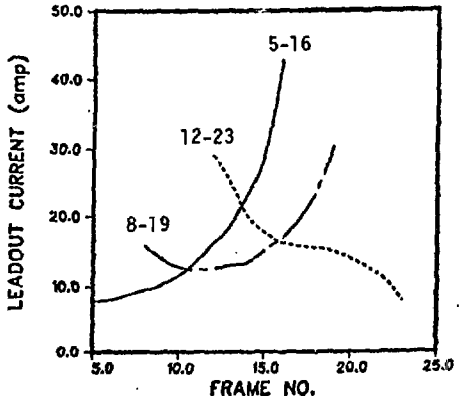

Fig. 10 Leadout current distribution for three power take-off locations (Total current= 200A in 12 frames. R = 0.5Ω, ṁ=3.2 kg/s, To=2825 K)

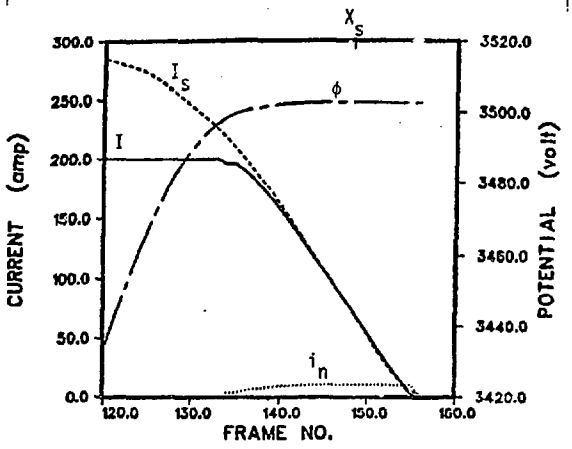

(a) I_1=200 at frame 134; I_2=0 at frame 156

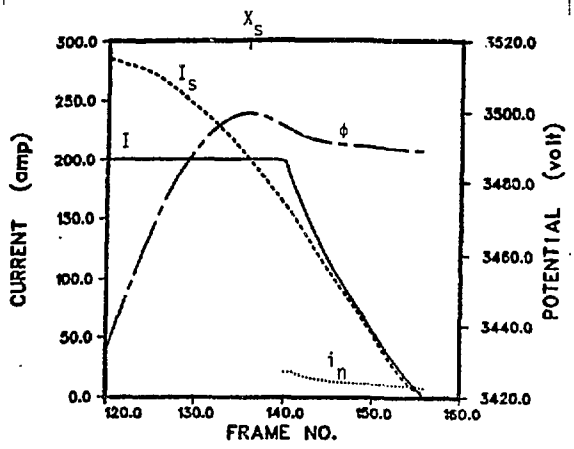

(b) I_1=200 at frame 140; I_2=0 at frame 156

Fig. 11 Behavior of the power take-off region with diodes and equal resistors (channel exit)

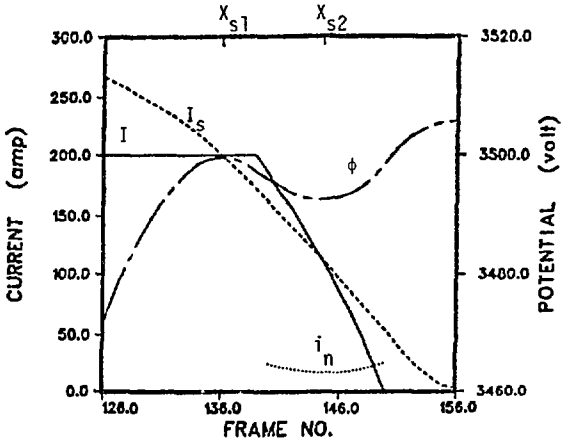

(a) I_1=200 at frame 140; I_2=0 at frame 150

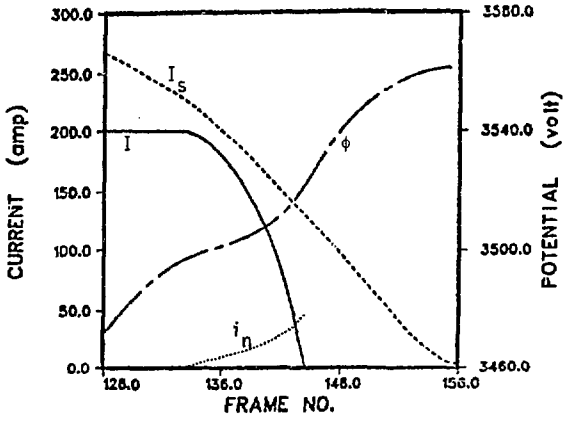

(b) I_1=200 at frame 132; I_2=0 at frame 143

Fig. 12 Behavior of the power take-off region with diodes and equal resistors (exit or intermediate section)

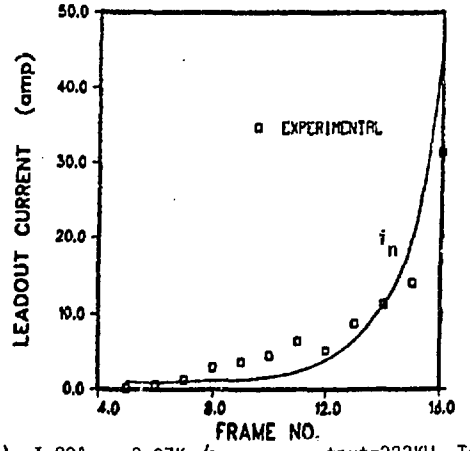

(a) I=90A, m=3.07Kg/s, power output=222KW, Test 4, measurement 2606

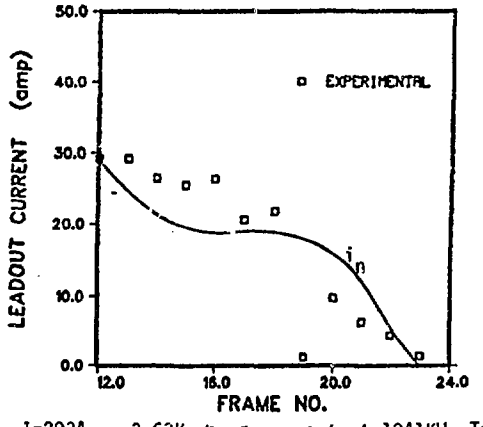

(b) I=203A, m=3.63Kg/s, power output=1041KW, Test 6, measurement 1135

Fig. 13 Current distribution at the inlet power takeoff region of the U-25B channel

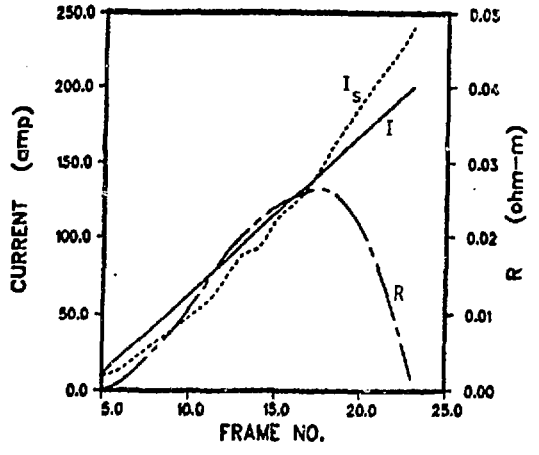

(a) resistance increases then decreases

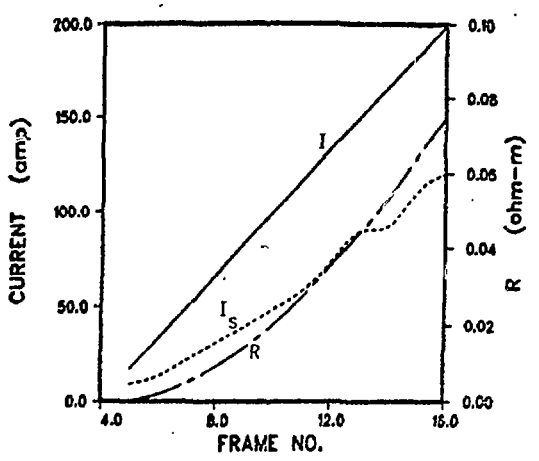

(b) resistance increases only

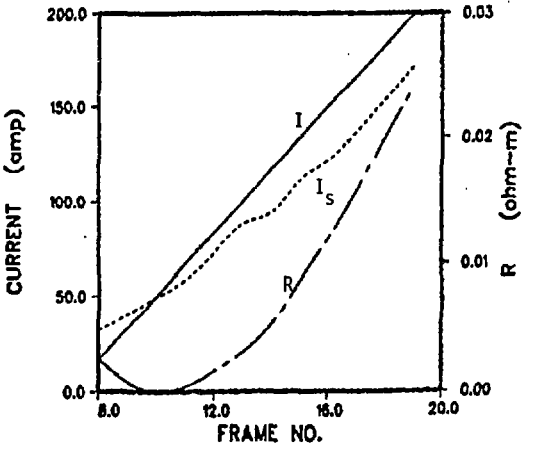

(c) resistance decreases then increases

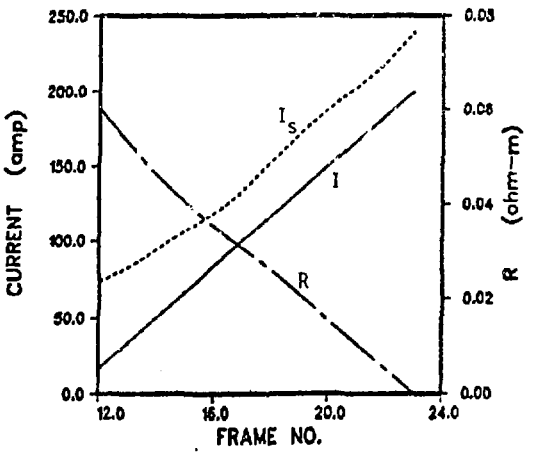

(d) resistance decreases only

Fig. 14 Typical resistance distribution for obtaining equal currents

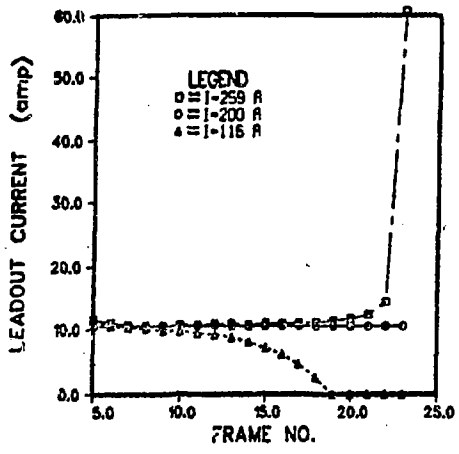

(a) resistance increases then decreases

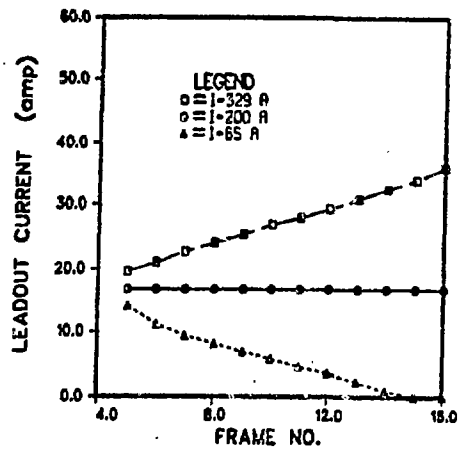

(b) resistance increases only

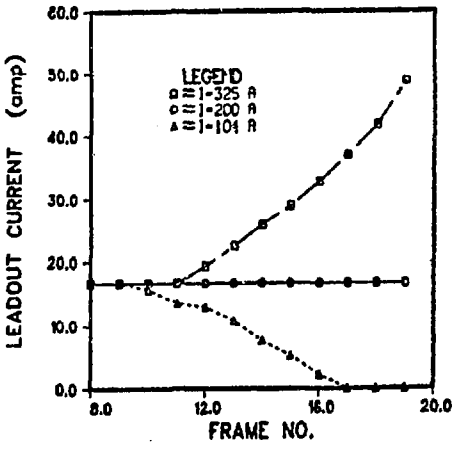

(c) resistance decreases then increasgs

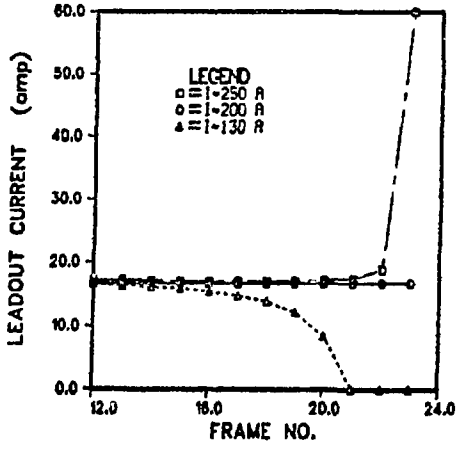

(d) resistance decreases only

Fig. 15 Leadout current distribution with variable resistors